Supporting Information for:

Conformal Hetero-Electrolyte Interface between Soft Oxyhalides and Garnet Enables Low-Pressure Lithium Reservoir-Free Solid-State Batteries

Max Palmer[Δc], Vipin K. Singh[Δa], Leonardo Merola[b], Karthikeyen Natarajan Pugazhendhi[a], Pallab Barai[d], Insang You[a], Yubo Wang[a], Eric Carlson[c], Cathy Wang[c], Hao Zheng[c], Venkat Srinivasan[d], Jürgen Janek[b], Jeff Sakamoto[c*], Linda F. Nazar[a*]

[a]*Department of Chemistry and the Waterloo Institute for Nanotechnology, University of Waterloo, N2L 3G1 Waterloo, Ontario, Canada*

[b]*Institute of Physical Chemistry and Center for Materials Research (ZfM), Justus-Liebig-University, Giessen, Heinrich-Buff-Ring 17, D-35392 Giessen, Germany*

[c]*Materials Department & Department of Mechanical Engineering, 1355 University of California, Santa Barbara, CA 93106-5050, United States*

[d]*Argonne National Laboratory, Lemont, IL, 60439, United States*

[Δ]*These authors contributed equally*

*lfnazar@uwaterloo.ca, *sakamoto@ucsb.edu

Supplementary material includes:

Experimental details/methods

Figure S1 to S30

Table S1 to S3

Experimental Details/Methods:

Materials

Mechanochemical synthesis of $LiTaOCl_4$ and $LiNbOCl_4$ (LTOC and LNOC)

The preparation of $LiTaOCl_4$ and $LiNbOCl_4$ were carried out using a mechanochemical route as reported previously by Tanaka et al.[1] The stoichiometric amounts of $TaCl_5$ or $NbCl_5$ (99.9%, Strem Chemicals) and LiOH (95%, Strem Chemicals), respectively, were taken. For the calculation of the stoichiometric amounts, a purity of 100% was assumed. The respective powders were transferred into an air-tight ZrO_2 milling jar (80 mL) containing ZrO_2 balls (70 g, 5 mm Ø). The reaction was conducted using a Fritsch Pulverisette 7 Premium ball mill for 16 cycles of 30 minutes of milling at 500 rpm, followed by a 30 minute rest to minimize excessive heating during homogeneous mixing. The final product was separated from the ZrO_2 balls using a Cole Palmer ASTME-11 standard test sieve (500 μm). Both LTOC and LNOC were obtained as white powders.

After milling, the resultant powders were collected and subjected to thermal treatment under an inert atmosphere. For $LiNbOCl_4$, annealing was performed at 100°C for 2 hours in a FB1415M furnace from Thermo Scientific. A ramp rate of 100 °C h^{-1} was applied until the dwell time, followed by natural cooling to room temperature.

$Li_3Al_3O_2Cl_8$ (LAOC)

Crystalline $LiAlCl_4$ was synthesized by using a stoichiometric mixture of LiCl (anhydrous, 99.95%, Fisher Scientific) and $AlCl_3$ (ultra-dry, 99.99%, Fisher Scientific) powders in a quartz tube under vacuum, followed by annealing at 200 °C for 20 h. During heating, the mixture melted into a liquid, which solidified upon cooling. The resulting $LiAlCl_4$ was ground into a fine powder for subsequent use. LAOC was prepared by hand-grinding stoichiometric amount of $LiAlCl_4$, $AlCl_3$, and $AlCl_3 \cdot 6H_2O$ (99%, Fisher Scientific) powders in the desired molar ratio for ~45 minutes, followed by annealing at 190 °C for 2 h under dynamic vacuum in a Büchi oven, connected to Schlenk line. HCl gas was released during this process. For this reason, the Büchi oven was connected to the liquid nitrogen pump through Schlenk line to condense HCl vapors generated during the process. $Li_3Al_3O_2Cl_8$ was synthesized via the stoichiometric reaction : $4.5LiAlCl_4 + 3.5AlCl_3 + AlCl_3 \cdot 6H_2O \rightarrow$ grinding and annealing $\rightarrow 3Li_{1.5}Al_3O_2Cl_{6.5} + 12HCl$.

Li_6PS_5Cl

The Li_6PS_5Cl (LPSCl, ~1μm) was purchased from NEI corporation. The LPSCl powder was used as received without further treatment.

$Li_{6.5}La_3Zr_{1.5}Ta_{0.5}O_{12}$ (LLZTO)

$Li_{6.5}La_3Zr_{1.5}Ta_{0.5}O_{12}$ (LLZTO) was synthesized following a solid-state synthesis. In summary, a 500 mL bottle was filled halfway by volume with 2 mm yttria-stabilized zirconia milling media

(MSE Supplies). Precursor powders of La_2O_3 (Pacific Industrial Development Corporation), ZrO_2 (Inframat Advanced Materials), and Ta_2O_5 (Inframat Advanced Materials) were added in stoichiometric amounts with 14 wt% excess of Li_2CO_3 (Sigma Aldrich) into the bottle. Approximately 110 mL of 200 proof ethanol was added. The mixture was milled for 20 hours and then dried. The results mixture was sieved to separate the milling media from the powder. The powder was then cold pressed into pucks. The pucks were calcined at 1000 °C for 4 hours under flowing dry air. After calcination the pucks were ground, sieved, and stored in an Ar-filled glovebox until further use. The powder was characterized with X-ray diffraction to confirm phase purity.

The LLZTO powder was densified through rapid induction hot-pressing following a previously reported procedure.[2] After densification, LLZTO billets were cut into 2.5 mm thick pellets and the edges were sanded until the diameter was 10 mm. The pellets were wet polished to a 0.1 μm finish with diamond paste.

Full cell materials

Uncoated single crystal $LiNi_{0.82}Mn_{0.07}Co_{0.11}O_2$ (NMC) and vapor-grown carbon fibers (VGCF, outer diameter = 30-80 nm) were purchased from MSE Supplies. The NMC and VGCF were dried at 120 °C under vacuum for 24 hours.

Methods

Surface treatment of LLZTO

Phosphoric acid, hydrochloric, acid and heat treatment of the LLZTO surface were chosen as cleaning steps as they are one of the most common treatments of LLZTO in the literature. They also demonstrate some of the most effective removal of the passivation layer.

Phosphoric acid treatment (H_3PO_4)

For symmetric cells, LLZTO pellets were submerged in 14.6 M H_3PO_4 for 1 min. The pellets were then rinsed with ethanol (100 %, Fisher Scientific) and acetone (> 99.5 %, Fisher Scientific), dried with a heat gun for 1 min, and then quickly transferred to an argon filled glove box. (O_2 < 0.1 ppm, H_2O < 0.5 ppm, Mbraun) after drying to prevent the rapid reformation of the passivation layer. For full cells, 5-6 drops of H_3PO_4 were dropped onto the exposed LLZTO side to be in contact with LNOC. After 1 minute the acid was dabbed with a Kimwipe and then wiped with ethanol and acetone.

Hydrochloric acid treatment (HCl)

LLZTO pellets were immersed in 1 M HCl for 6 minutes, then gently wiped with Kimwipes to remove any residue and dried with a heat gun for 30 seconds. Immediately after drying, the cleaned pellets were transferred to an argon-filled glovebox. The bilayer symmetric cells were assembled within 2 minutes, as we observed that passivation layers begin to reform on the LLZTO surface after

2-3 minutes even under argon atmosphere which leads to irreproducible data. The detailed analysis for acid treatment is given in **Table S3** and **Fig. S13**.

Heat treatment (HT)

After polishing, the pellets were transferred into the argon-filled glovebox (O_2 < 0.1 ppm, H_2O < 0.5 ppm, Mbraun) in less than 30 seconds. For bilayer symmetric cells the pellets were further polished inside the glovebox using P1000 grit sandpaper and the surface was cleaned with a blower. Finally, the pellets were vacuum sealed inside the quartz tube and annealed in a muffle furnace at 400°C for 3 hours with 300 ºC/ h heating rate followed by natural furnace cooling.

Ultrasonic measurements

Measuring the Young's, bulk, and shear moduli were attempted using the ultrasonic acoustic technique. 100 mg of LNOC and LTOC and 60 mg of LAOC were cold pressed at 370 MPa for 5 minutes in a 6.35 mm die. To determine the longitudinal and transverse velocities, ultrasonic measurements were performed using an Olympus Model 5073PR receiver in the pulse-echo method. All measurements were conducted in an argon filled glove box. Pulses were transmitted and received with a 5 MHz center frequency transducer (Olympus). The samples were coupled to the transducer in longitudinal and transverse modes with the Echo Pure medium viscosity couplant and Echo shear wave couplant from Echo Ultrasonics, respectively. Measurements were performed in triplicate for LNOC and LTOC and duplicate for LAOC and the reported values are the average. Poisson's ratio and moduli were calculated using the formulas

$$Poisson's\ ratio, \nu = \frac{{V_L}^2 - 2{V_T}^2}{2{V_L}^2 - 2{V_T}^2}$$

$$Shear\ modulus, G = p{V_T}^2$$

$$Young's\ modulus, E = \frac{p{V_L}^2(1+\upsilon)(1-2\upsilon)}{1-\upsilon}$$

$$Bulk\ modulus, K = \rho\left(\frac{3v_L^2 - 4v_T^2}{3}\right)$$

$$\rho = density, v_L = longitudinal\ velocity, v_T = transverse\ (shear)\ velocity$$

The ultrasonic waveforms, moduli, and Poisson ratio values are reported in **Fig. S5** and **Table S1**. It can be observed that the Poisson ratio for LTOC and LNOC are atypically low whereas the measured value for LAOC is a more realistic value. This may be due to residual porosity within the LTOC and LNOC pellets that act as a source for ultrasonic wave reflections instead of the expected

back wall of the pellet. Premature wave reflection would lower the measured moduli. The values are included for transparency although the LTOC and LNOC values may be unreliable.

Work of compression measurements

An appropriate amount of LAOC, LTOC, LNOC, and LPSCl powder was added into a 6 mm diameter die to yield a densified pellet with a thickness of 2 mm assuming 100% relative density. This corresponds to a mass of 0.1172 g, 0.1932 g, 0.1653 g, and 0.1039 g for LAOC, LTOC, LNOC, and LPSCl, respectively. The loaded die was sealed in an air-tight plastic bag and transferred to a universal tester (Instron, model 5950). The die was compressed at 200 kgf/min up to 1000 kgf (~310 MPa). The area under the force-displacement curve was integrated using the OriginPro software.

Hardness measurements

100 mg of LAOC, LNOC, LTOC, and LPSCl were cold pressed at 370 MPa for 5 minutes in a 10 mm die. Pressed pellets were then put into an epoxy mold (Epoxi Cure 2, JH Technologies) for polishing. The pellets in epoxy were then hand polished up to 10,000 grit. Microindention hardness measurements were performed on a Mitutoyo HM-112 instrument with a load of 0.4903 N and a dwell time of 5 seconds. Prior to measurement the epoxy molds were covered in a thin layer of white mineral oil to avoid air exposure. 10 indents were made on each sample. The diagonals of the indents were measured with a VK-X3050 laser confocal microscope (Keyence). The LNOC and LTOC were measured at 50x magnification and the LAOC was measured at the 20x magnification as the indent was outside the viewing window of the 50x lens. Microindention hardness was calculated as

$$Hv = \frac{0.1891F}{d^2}$$

where F is the load in N and d^2 is the average of the indent diagonals. Hv was then converted into SI units by multiplication of standard gravity.

<u>Fabrication of symmetric cells</u>

Cell A (Au|LLZTO|Au and Li|LLZTO|Li)

For ionic conductivity measurements, the polished LLZTO pellets were coated on both sides with 8 mm diameter gold (Au) electrodes (Angstrom Thermal Evaporator) serving as blocking contacts. The Au-coated pellets were assembled in a pouch cell configuration with nickel tabs in direct contact with the gold layers (Ni|Au|LLZTO|Au|Ni) to act as current collectors. The pouch cell was then sealed inside the Ar-glovebox to prevent atmospheric exposure.

To evaluate the interfacial stability of the Li|LLZTO interface, 6 mm-diameter lithium foil (99.9%, Goodfellow; 100 μm thickness) was freshly scraped with a ceramic knife to remove surface oxides and adhered to the center of a 10 mm copper foil. These Li-Cu electrodes were placed on both sides of the surface-treated LLZTO pellet to form a Cu|Li|LLZTO|Li|Cu stack. The assembly was

then isostatically pressed at 450 MPa for 45 min to ensure low resistance at the Li-LLZTO interface.[3] For both ionic conductivity and interfacial stability impedance measurements, the pouch cells were mounted on a pressure-controlled frame equipped with a force sensor (Mouser electronics, Ltd.)

Cell B (LMOC|LLZTO|LMOC)

For this typical procedure, 180 mg of solid electrolyte powder was loaded on both sides of the surface-treated pellet in the PEEK mould and sandwiched in between two stainless-steel pins and

Scheme 1

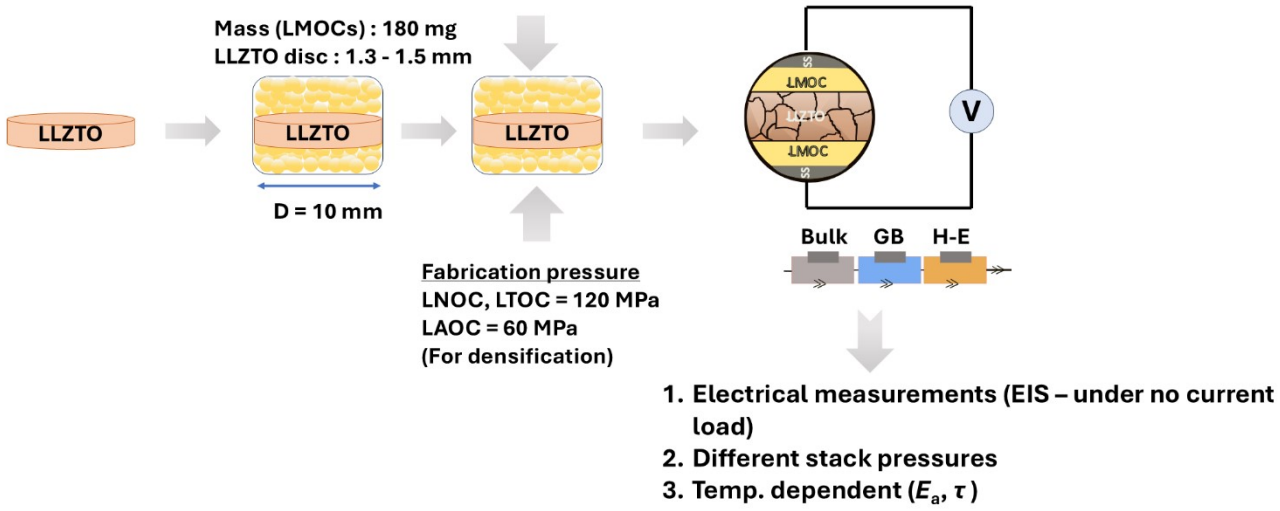

pressed under 120 MPa to densify the LMOCs against the LLZTO pellet. The assembled cell was then placed in an aluminum frame equipped with the force sensor (Mouser electronics. Ltd.) and for EIS measurements at different stack pressures.

Full Cell Assembly

After heat treatment, Li foil (200-300 □m thick) was scraped until shiny. An 8 mm diameter disk was punched out and compressed onto one side of the LLZTO pellet at 70 lbf for 30 seconds. The Li|LLZTO was then loaded into a custom fixture and heated to 170-175 °C under ~1 MPa stack pressure for at least 12 hours. The custom built fixture has a primarily stainless steel body that houses the Li|LLZTO construct, stainless steel rods to control the pressure, and PTFE to help align the rods. After forming the Li|LLZTO interface, the bare LLZTO side was acid washed with 85 wt% H_3PO_4 for 1 minute. The H_3PO_4 was dabbed with a Kimwipe and then the residual acid was wiped off with a Kimwipe wet with acetone and dried with a heat gun.

NMC, LNOC, and VGCF were hand mixed in a mortar a pestle for 10 minutes in a weight ratio of 66.5 : 28.5 : 5 to make the cathode composite. For the 2 wt% VGCF cell, the recipe was 68: 30: 2. 75-80 mg of LNOC was first added to a 10 mm diameter polyetheretherketone (PEEK) die and compressed at 100 MPa for 1 minute with stainless-steel pins to form the LNOC interlayer. Prior to densification the stainless-steel pins were sanded with 1500 grit ANSI sandpaper and then

sonicated in 200 proof ethanol following our previous work.[4] Next, 11-12 mg of cathode composite was added onto the LNOC interlayer, spread around, and then densified at 370 MPa for 3 minutes. The assembled Li|LLZTO half-cell was then added to the bare LNOC side. 3 pieces of 3/8" grafoil was placed behind the nickel foil. The cell was loaded into an Imada load frame and compressed to 7 MPa stack pressure. The cell was then heated to 80 °C for 16 hours and then the temperature was lowered to 60 °C. Galvanostatic cycling was carried out between 2.8 - 4.3 V (vs Li^+/Li) with one activation cycle at C/10 and extended cycling at C/5 (1 C = 200 mA/g). The impedance data at 100% state of charge was fit with a *R(RQ)(RQ)(Ws)* model.

Ag|LLZTO Preparation

For silver (Ag) Li free cells, Ag was sputtered with the Denton Desk V onto polished LLZTO for 20 minutes under a chamber pressure of 80 mTorr yielding a thickness of ~100 nm. The thickness of the Ag film was determined with a laser confocal microscope. To assemble Li|LLZTO|Ag cells, the LLZTO|Ag was heat treated at 400 °C for 3 hours in an argon filled glove box. Next, Li was added and conditioned onto the other LLZTO side as previously described. The Li|LLZTO|Ag was added to a PEEK die and then heated to 60 °C and compressed 7 MPa. Galvanostatic stripping and plating current were carried out following the same procedure of the full cell. The cut off voltages were -1 and 1 V for plating and stripping, respectively. 2 mAh cm^{-2} was plated each cycle to match the areal capacity of the full cell cathode composite.

For full cells, the Ag|LLZTO was prepared in the same manner but instead of conditioning Li to the other LLZTO side, it was added directly to the densified NMC|LNOC construct. Then, 8 μm thick and 10 mm diameter copper foil was placed behind the Ag followed by 3 layers of 10 mm diameter grafoil. The copper foil was cleaned with 200 proof ethanol prior to addition to the full cell.

Improved Coulombic efficiency in Li|LLZTO|Ag cells

As there was residual Li after the activation cycle, the increase in Coulombic efficiency from the C/10 cycle to C/5, this may be due to the Ag seeds transforming into a Li-rich Li-Ag alloy: the activation cycle lost ~0.054 mAh cm^{-2} of Li. With 1 mAh cm^{-2} equating to a thickness of 4.9 μm, this corresponds to a thickness of 265 nm of Li. The moles of each element can be determined with the element's molar volume (V_m). The molar volume of Li and Ag at this pressure and temperature is not known and thus the molar volume at room temperature of atmospheric pressure was chosen ($V_{m,\,Li}$ = 1.3 x 10^{22} nm^3 and $V_{m,\,Ag}$ = 10.27 x 10^{22} nm^3).[5] This implies a mole ratio of Li/Ag = 20.9. Therefore, after the activation cycle, the remaining interlayer is a $Li_{21}Ag$ alloy. Work by Thomas et al. determined that Li-rich Li-Ag alloys will have higher Li^+ diffusion coefficients than Li-poor Li-Ag alloys.[6] Therefore, the activation cycle "activates" the Ag seeds by lithiating them.

Electrochemical Characterization

The potentiostatic electrochemical impedance spectroscopy (PEIS) was carried out using a Biologic-SP200 potentiostat with a frequency range of 7 or 3 MHz to 100 mHz and 10 mV sinus amplitude. Arrhenius measurements were performed in the GWS benchtop humidity chamber from -50 °C to +30 °C. Further, the data was examined using the RelaxIS 3 software and DRT plots were calculated using the Gaussian base function with a value of 0.001. Distribution of relaxation times (DRT) analyses were performed with a Gaussian basis function and a second order derivative (shape factor: 0.5) and $l = 10^{-3}$ within a frequency range between 3 MHz and 1 kHz considering the complex data set.

Physical Characterization

X-ray Diffraction (XRD) and Scanning Electron Microscopy (SEM)

XRD data were collected using the zero-background silicon holder using PANalytical Empyrean instrument (Cu-Kα radiation (λ = 1.5405Å)) with a PIXcel 2D detector operating under 45 kV voltage and 40 mA current. SEM studies were conducted in a Hitachi SU8700 FESEM instrument to obtain the morphology and to visualize the density of the pellet. The relative density of the sintered pellets was determined using Archimedes' principle with a custom-built density measurement setup, employing a Sartorius ED124 analytical balance for precise mass measurements in both air and solvent (ethanol) to ensure accurate density calculations.

X-ray Photoelectron Spectroscopy (XPS)

XPS measurements of pristine and treated LLZTO pellets were performed using a PHI VersaProbe 4 instrument (Physical Electronics GmbH, Germany) equipped with a monochromatic Al-Kα radiation source ($h\nu$ = 1486.6 eV). Charge neutralization for the electronically insulating LLZTO pellets was achieved using a combination of low-energy argon ion and electron guns. The samples were mounted on the XPS holder using non-conductive double-sided adhesive tape inside the Ar-filled glovebox (O_2 < 0.1 ppm, H_2O < 0.5 ppm, Mbraun) and transferred to the XPS chamber with an air-free transfer chamber (Leica Systems, Germany).

As previously reported, the X-ray source operated at 50 W, producing a 200 μm diameter beam.[7] The measurement chamber pressure was maintained between 10^{-7} and 10^{-6} Pa. Survey spectra were acquired with a pass energy of 224.0 eV and a resolution of 0.5 eV·step^{-1}, while core-level spectra (O1s, C1s, Li1s, La3d, Zr3d, Al2p) were recorded with a pass energy of 55.0 eV and a resolution of 0.2 eV·step^{-1}. Spectra were calibrated to the adventitious carbon C1s signal at 284.8 eV.

Data analysis was conducted using CasaXPS (version 2-3-26PR1.0, Casa Software Ltd). A Shirley background and GL (30) line shapes were applied for signal fitting.

Focused Ion Beam-Scanning Electron Microscopy (FIB-SEM)

Cross sectional analysis was conducted using a Helios 5 PFIB UXe Dual Beam Plasma - FIB. The process involves the deposition of solid carbon using an electron beam (13 nA, 5 kV) to protect the surface of the sample. Next, a layer of solid tungsten was deposited on top of the carbon layer using an ion beam (0.43 nA, 30 kV) to minimize curtaining effects caused by surface roughness. Following this, rough ion milling was performed directly below the deposition using a high ion current of 65 nA at 30 kV. To further refine the cross-section and remove curtaining and redeposition artifacts, smaller ion currents of 9.3 nA and 2.5 nA at 30 kV were used for cleanup. The sample was then imaged using conventional SEM parameters (0.8 nA, 5 kV). Finally, high-resolution imaging was conducted in immersion mode of the SEM column (2 kV, 25 Pa) at the required magnifications. SEM images were analyzed with *ImageJ*.

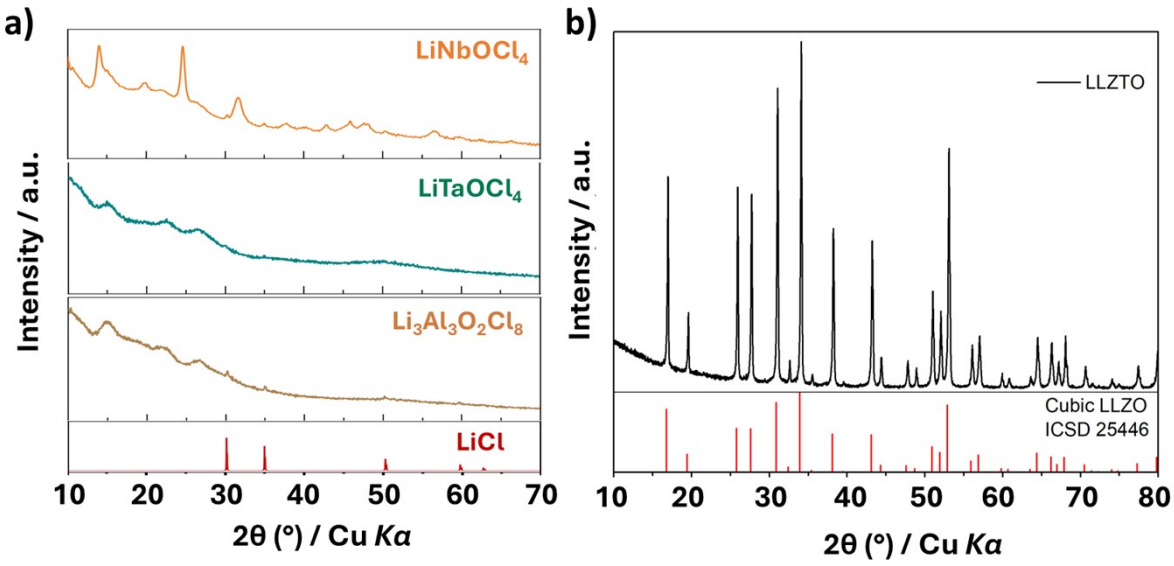

Figure S1*: Powder XRD of a) LMOCs (M=Nb, Ta, Al) and b) LLZTO.*

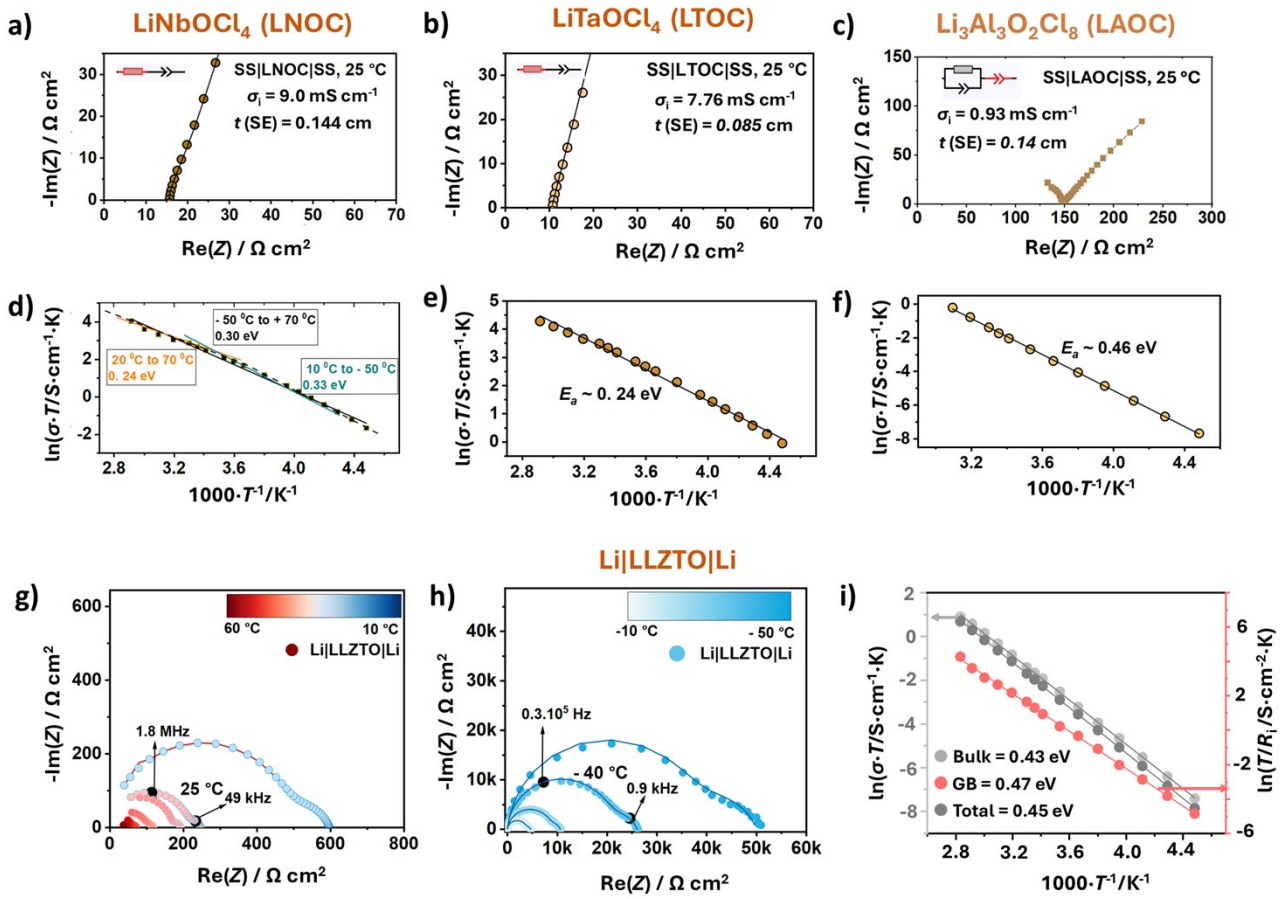

Figure S2. *Electrical properties of oxyhalide solid electrolytes. (a,b,c) Nyquist plot at 25 ºC for LNOC, LTOC and LAOC; (d,e,f) corresponding E_a values, LNOC, LTOC and LAOC; (g,h) Nyquist plots of Li|LLZTO|Li at different temperatures and (i) corresponding E_a plot.*

Figure S2 g-i) show the Nyquist plot and Arrhenius of the Li|LLZTO|Li cells. For this cell setup, the interface was prepared by heat treatment of LLZTO at 420 °C to remove the passivation layer followed by high pressure (i.e., 450 MPa - see methods SI), the Li|LLZTO interfacial contribution vanishes as there is no visible contribution, even at -40 °C (**Fig. S2h**). Similar low interfacial resistance values were previously reported by Sharafi et al.[8] for bare Li|LLZTO interfaces after conditioning at 175 °C. The corresponding Arrhenius plots for Li|LLZTO|Li cells show only bulk transport and grain boundary charge transfer in LLZTO, allowing clear deconvolution of these processes in LMOC|LLZTO|LMOC (M=Nb, Ta) symmetric configurations.

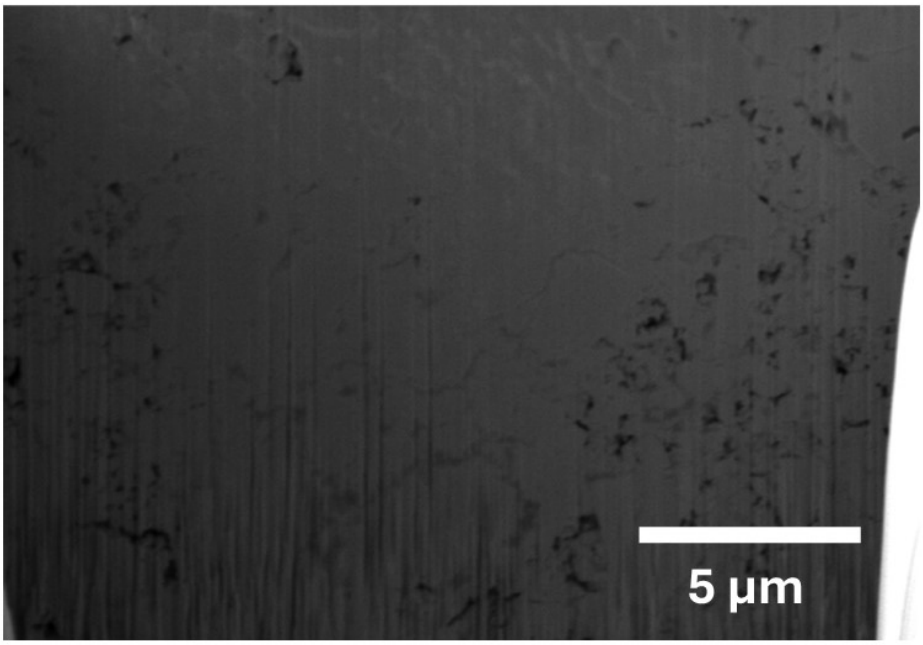

Figure S3*: FIB-SEM of LTOC after 120 MPa densification pressure for 3 minutes. The 10 mm PEEK die was used to carefully remove the pellet after densification.*

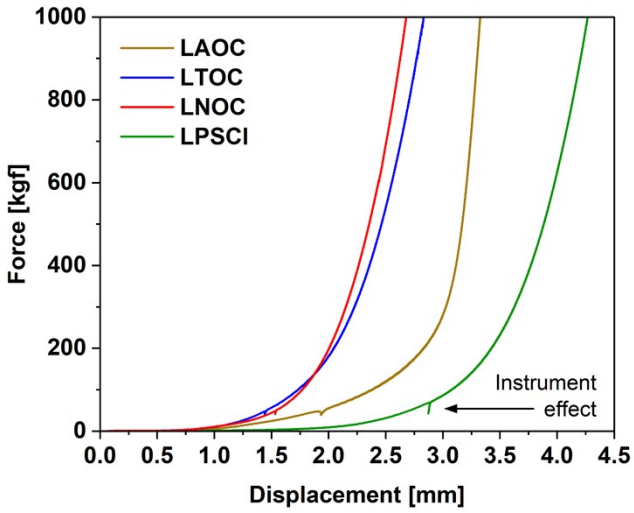

Figure S4*: A representative force-displacement curve of LAOC, LTOC, LNOC, and LPSCl.*

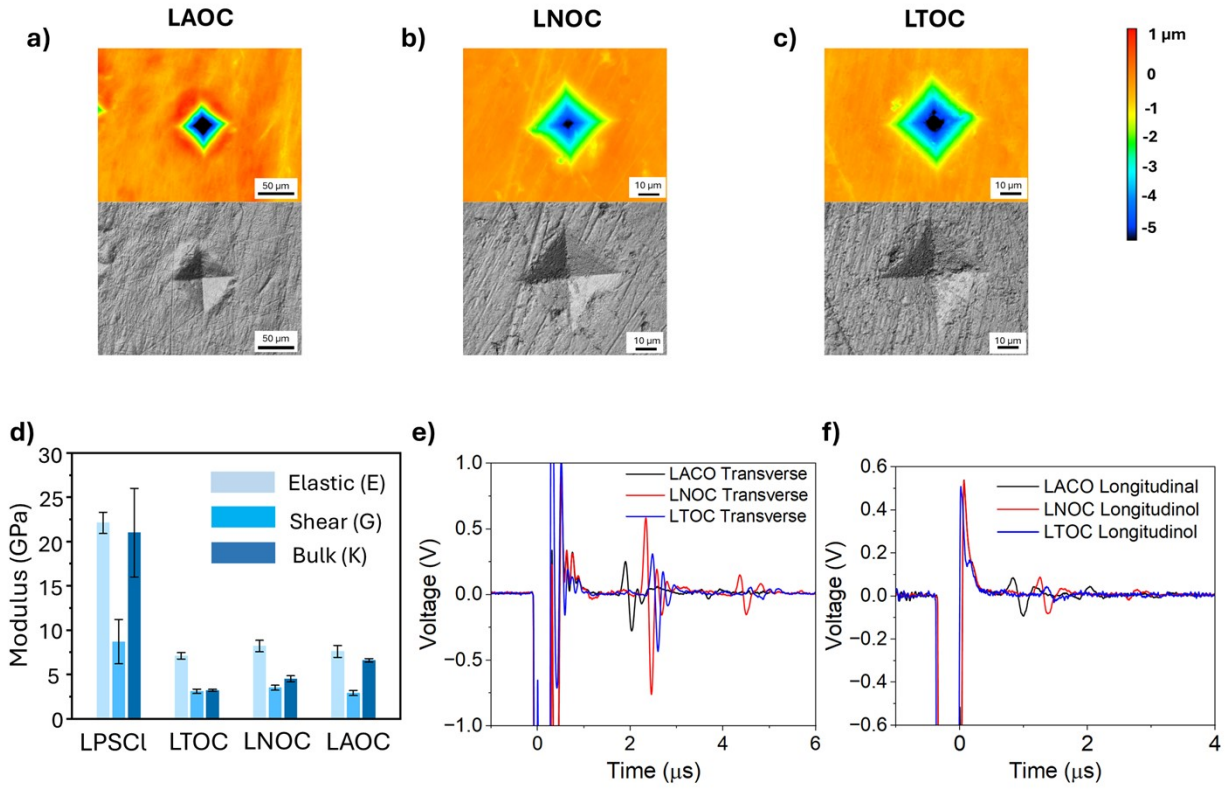

Figure S5*: a,b,c) Indentation maps of LAOC, LNOC and LTOC, d) Modulus measurements, LPSCl values are retrieved from the literature.[9] e,f) Representative waveforms for LNOC, LTOC, LAOC – pulse-echo, longitudinal transducer.*

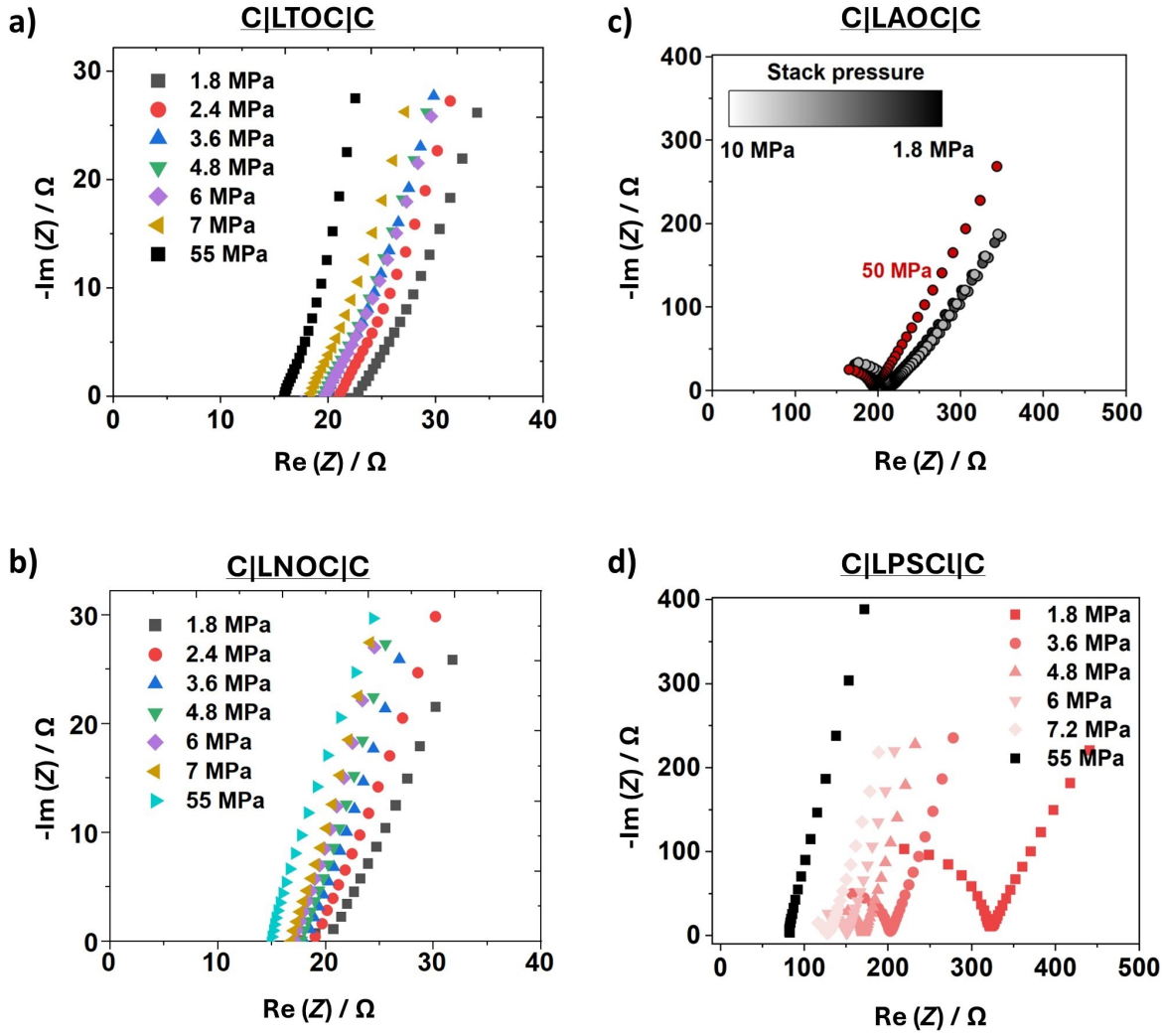

Figure S6*: (a,b,c) Ionic conductivity of LTOC, LAOC and LNOC; (d) LPSCl at different stack pressure. The fabrication pressure used for densification was 120 MPa for 3 minutes. Thickness of LNOC = 0.097 cm, LTOC = 0.1 cm, LPSCl = 0.16 cm, LAOC = 0.18 cm after 120 MPa densification pressure. Similar thickness values were considered to determine the ionic conductivity at released low stack pressures. Equivalent circuit used for C|LTOC|C, C|LNOC|C : (R)-(Q) in series, and for C|LAOC|C, C|LPSCl|C : (R)-(R)(Q)-(Q).*

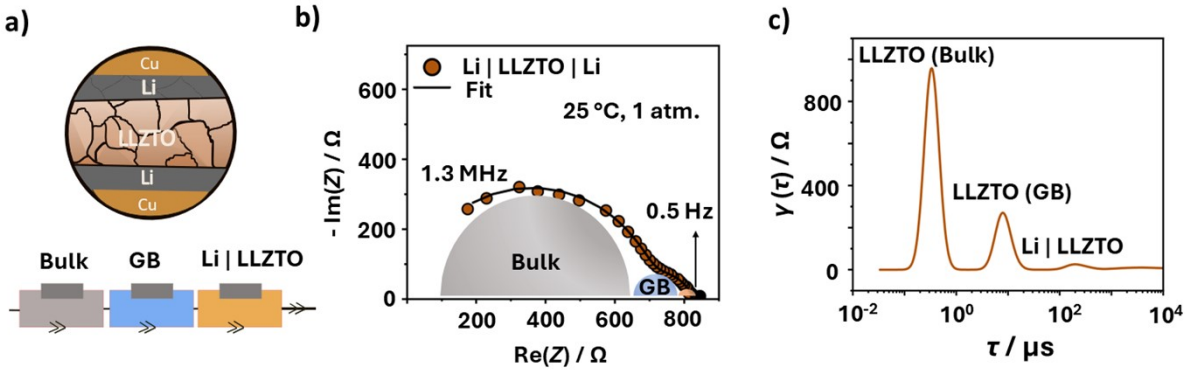

Figure S7: *(a) Cell schematic of Li|LLZTO|Li symmetric cell (reference); (b) Nyquist plot at 25 °C showing a separate contribution of bulk and grain boundary of LLZTO, and (c) corresponding DRT map - including distinct bulk, GB regions and negligible interface-related contribution (<5 Ω cm²). The Nyquist plot was fitted with an (RQ)-(RQ)-(RQ)-(Q) equivalent circuit in series.*

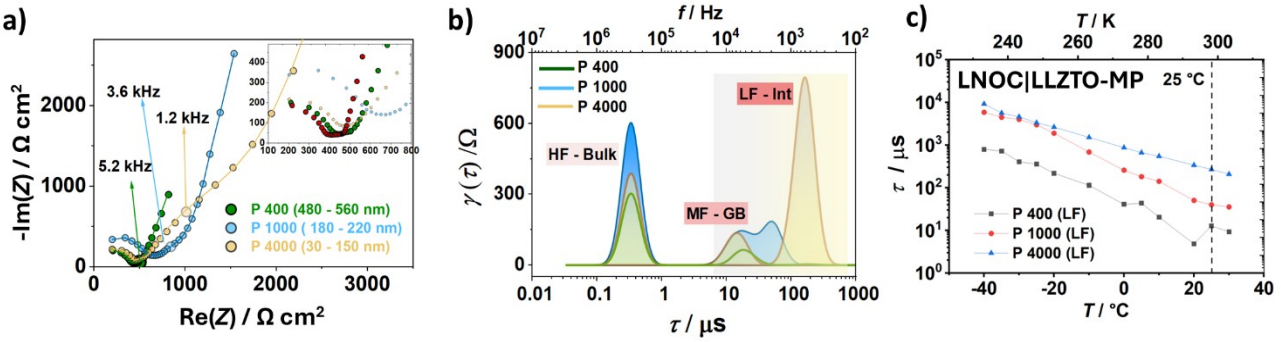

Figure S8*: (a) Nyquist plots showing the effect of mechanical polishing for LLZTO discs, (b) corresponding DRT plots, (c) temperature-dependent average time constant values. Measurements were performed at 55 MPa and 25 °C with a LNOC|LLZTO|LNOC bilayer symmetric cell and the powder-to-pellet method. P 400 (Sq ~ 300 nm), P 1000 (Sq: 120-150 nm), and P 4000 (Sq ~ 30 nm) indicated different grit-size SiC sandpapers, with root-mean-square (Sq) values indicated. The Nyquist plots were fitted with a (RQ)-(RQ)-(RQ)-(Q) equivalent circuit. The first three (RQ) elements were assigned to the $LLZTO_{Bulk}$, $LLZTO_{GB}$, and the H-E interface, followed by the blocking tail fitted with a single constant phase element (Q).*

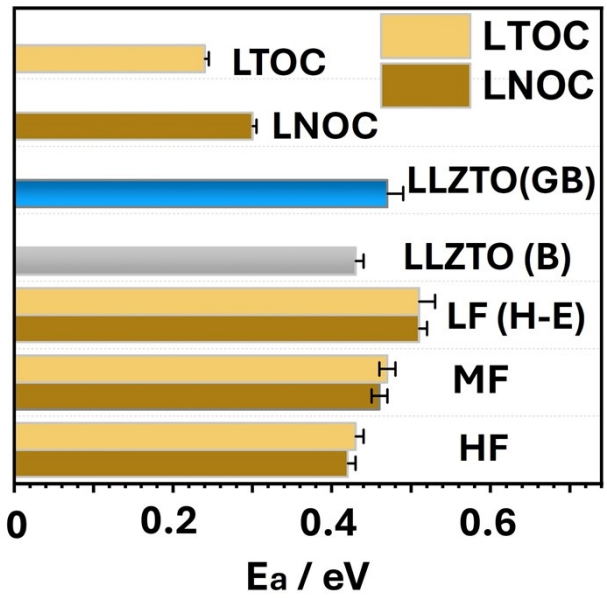

***Figure S9**: Summary of activation energy values for different contributions in bilayer symmetric cells with standard deviation from 3 different cells.*

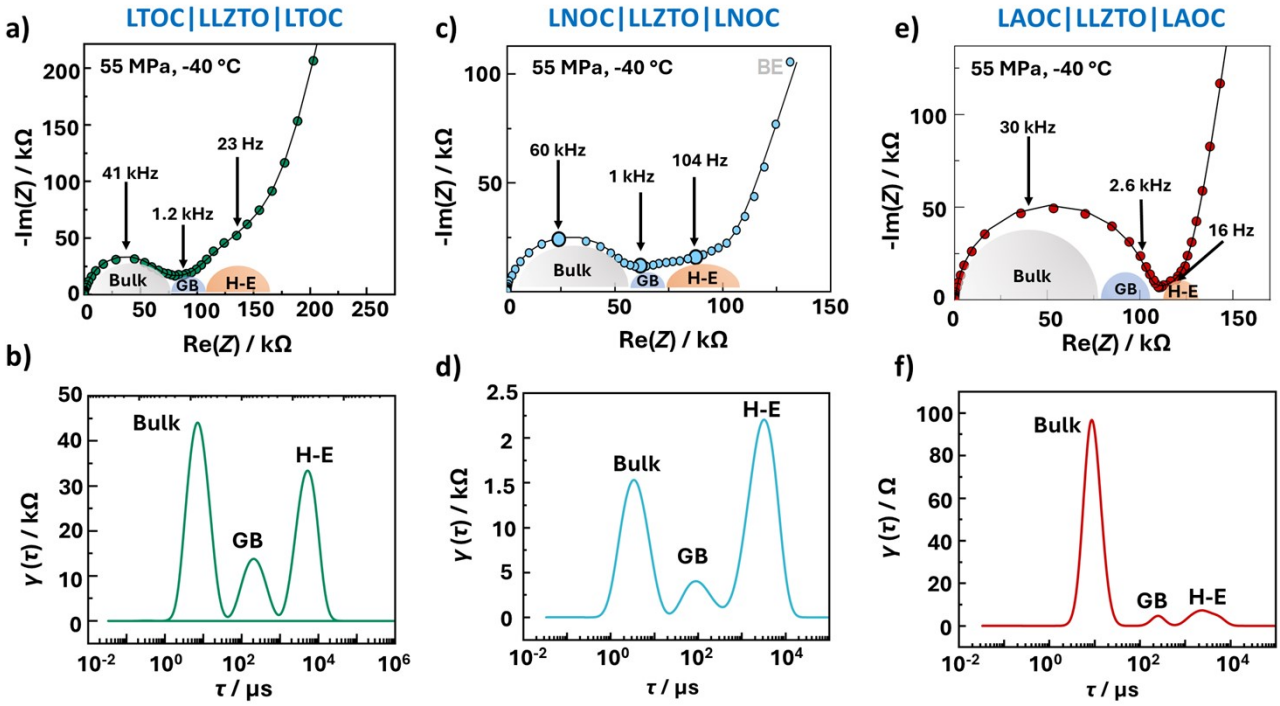

***Figure S10**: (a,b,c) Nyquist plots of bilayer symmetric cells at -40 °C and 55 MPa and their corresponding (b,d,f) DRT plots. The Nyquist plots were fitted with a (RQ)-(RQ)-(RQ)-(Q) equivalent circuit.*

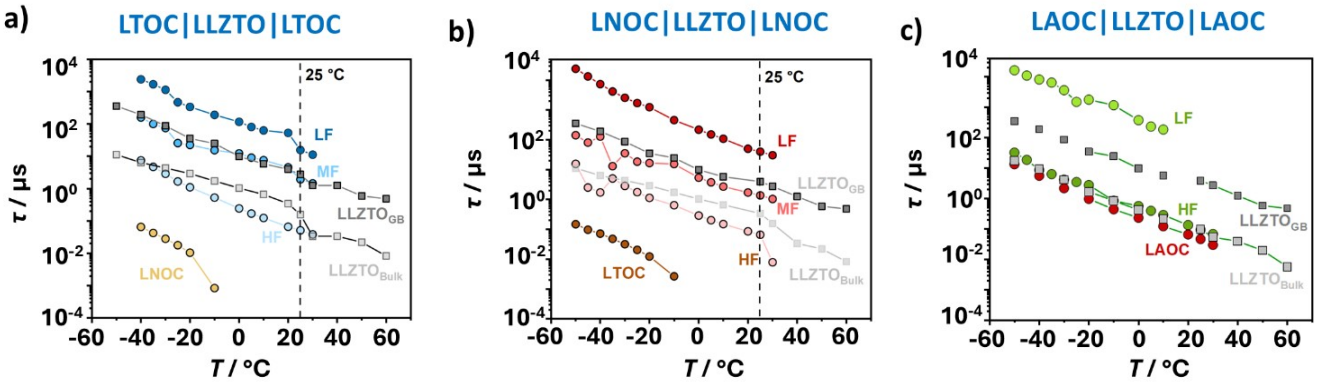

***Figure S11**: Temperature dependent average time constant measurements of bilayer symmetric cells (a) LTOC|LLZTO|LTOC, (b)LNOC|LLZTO|LNOC and (c) LAOC|LLZTO|LAOC at 55 MPa. The dashed lines serve as guidance for the reader's eye, rather than the linear fitting.*

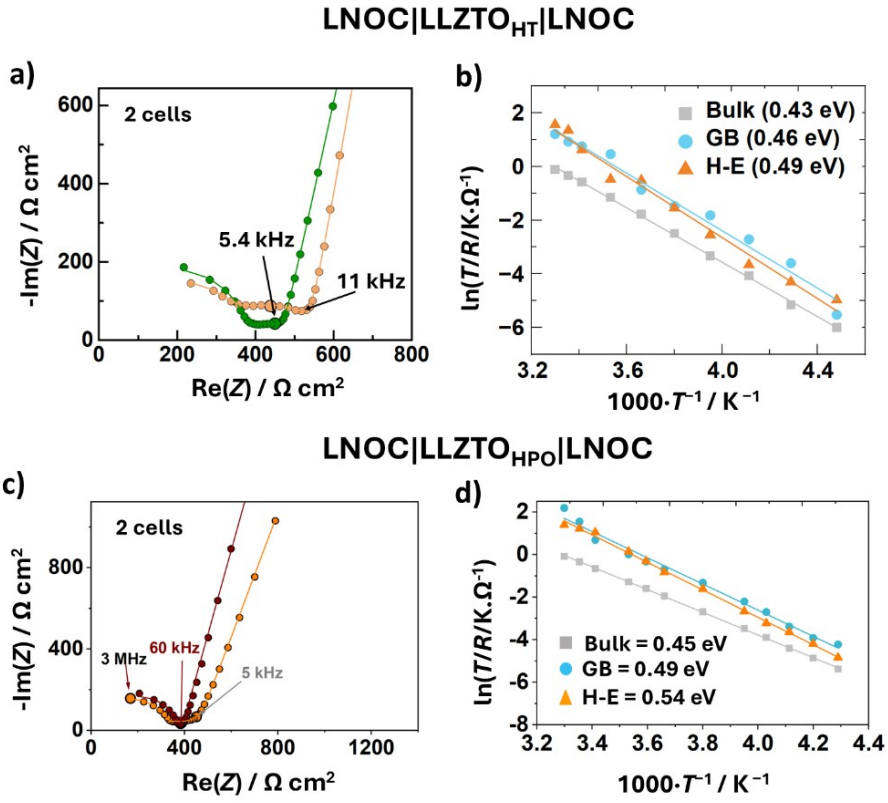

***Figure S12:** Effect of LLZTO surface treatment – bilayer symmetric cell (LNOC|LLZTO|LNOC) after heat treatment and H_3PO_4 treatment, a,c) Nyquist plots, and b,d) Arrhenius plots to determine the activation energy. All measurements were performed at a pressure of 55 MPa. The Nyquist plots were fitted with a (RQ)-(RQ)-(RQ)-(Q) equivalent circuit.*

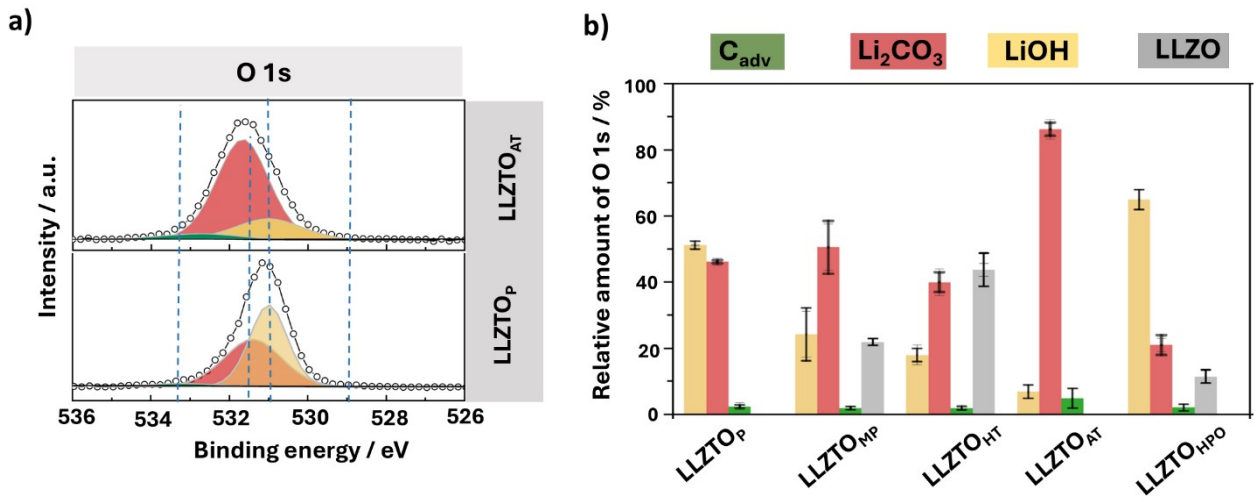

***Figure S13**: a) O 1s spectra of the LLZTO discs after 1 M H-Cl acid treatment (LLZTO$_{AT}$), and LLZTO$_P$ denotes the pristine (reference), b) Comparison of the relative amount of each component of the O 1s detailed spectra. C_{adv} denotes adventitious carbon.*

Figure S13a depicts the O 1s XPS spectrum of a polished LLZTO disc immersed in 1 M HCl for 6 min. The results indicate that acid treatment is ineffective at removing surface contaminants, as the treated surface remains dominated by LiOH and Li_2CO_3. The high level of residual contaminants after HCl exposure is consistent with some literature reports, although others have observed significantly cleaner LLZO surfaces following acid treatment.[10,11] Notably, among all surface treatments discussed so far, acid treatment results in the highest H-E interfacial resistance and the largest standard deviation (**Table S3**). This behavior further supports the re-formation of passivation layers, as evidenced by the high activation energy (0.56 eV) of the H-E interface.

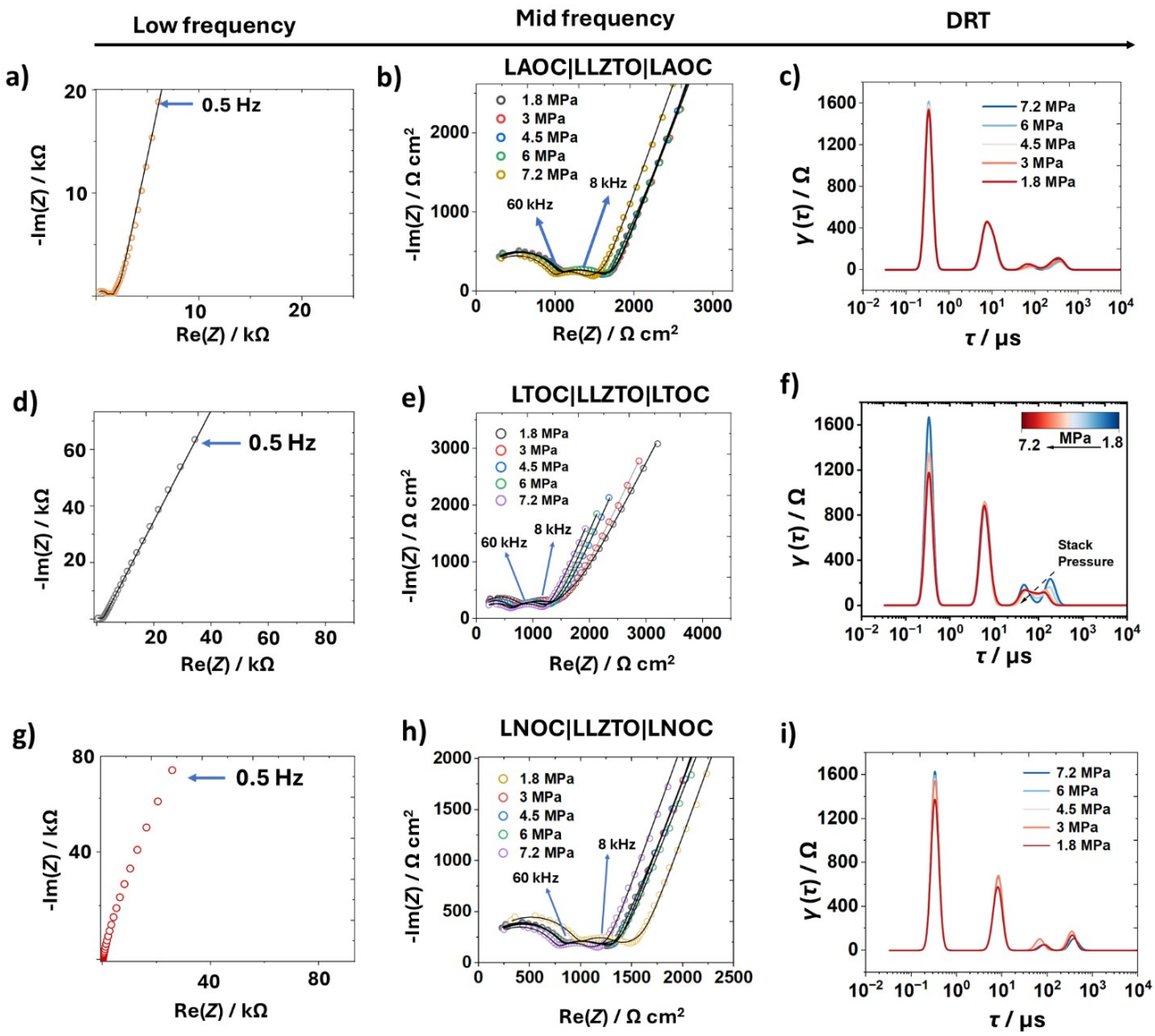

Figure S14: *Nyquist plots showing the evolution of H-E resistance under low stack pressure regime (i.e., 1.8 to 7.2 MPa) for bilayer symmetric cells and corresponding DRT maps (a,b,c) C|LAOC|LLZTO|LAOC|C, (d,e,f) C|LTOC|LLZTO|LTOC, and (g,h,i) C|LNOC|LLZTO|LNOC|C. Equivalent circuit used to fit the Nyquist plots : (RQ)-(RQ)-(RQ)-(Q)*

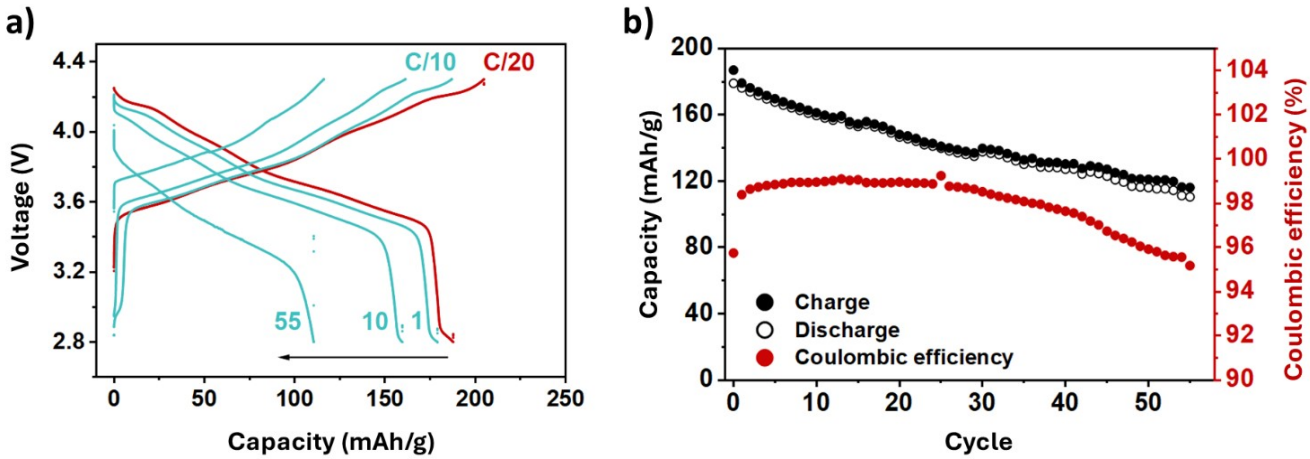

***Figure S15**: A NMC|LNOC|LLZTO|Li full cell with 2 wt% VGCF and an areal capacity of 2 mAh cm^{-2} at 60 °C under 7 MPa stack pressure. The Li|LLZTO$_{HT}$ interface was prepared with the "cold isostatic press" at 380 MPa for 40 minutes to remove geometric current constriction at the Li|LLZTO interface. The cathode side was prepared by the "powder-to-pellet" approach where LNOC (180 mg) powder was hand pressed on the surface of LLZTO followed by the final densification of cathode composite at 120 MPa for 3 minutes.*

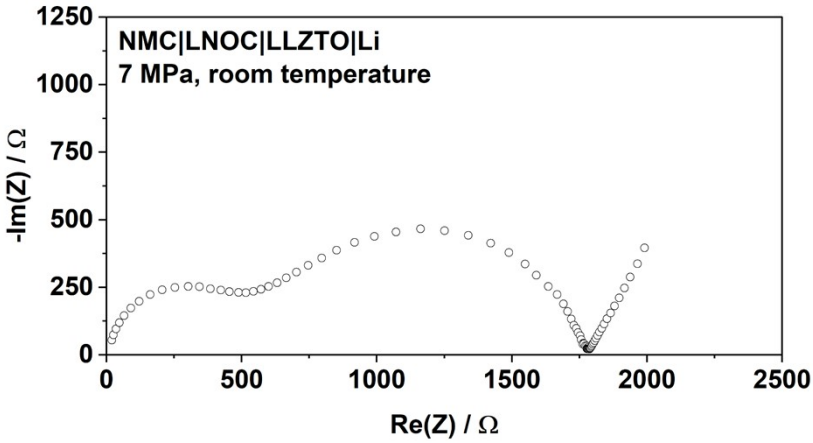

***Figure S16**: Full cell at room temperature right after assembly showing a large cell resistance due to constriction resistance at the LNOC|LLZTO interface.*

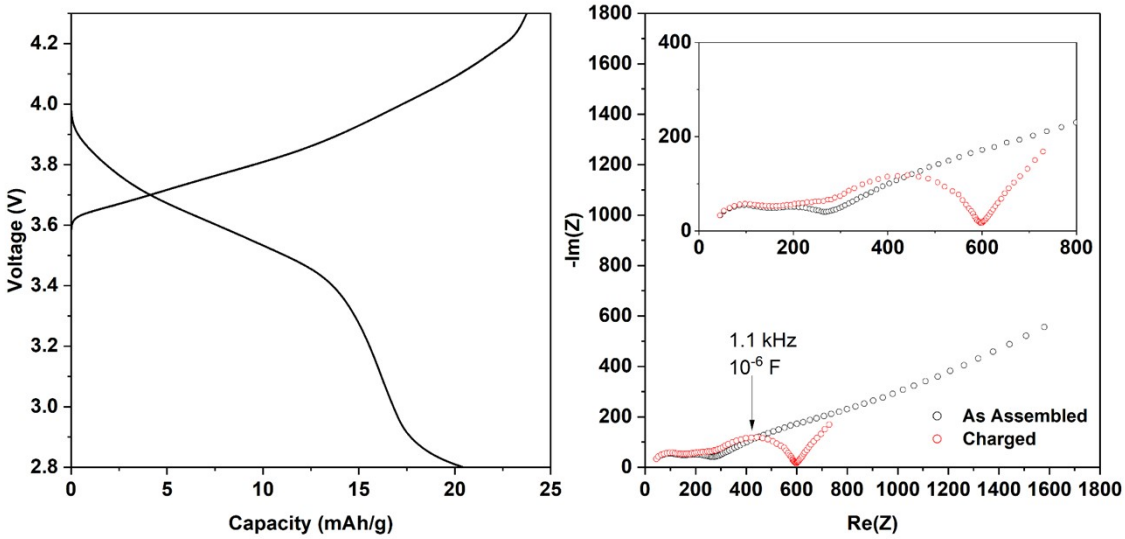

***Figure S17**: A NMC|LNOC|LLZTO|Li with 0 wt% VGCF. a) Galvanostatic cycling at a C/20 rate. Even at C/20 the cell can only discharge 20 mAh g^{-1}. c) Nyquist plots of the as assembled cell and after charging to 4.3 V. After charging to 4.3 V a semicircle appears at 1.1 kHz with a capacitance on the order of 10^{-6} F. This process is assigned to the electronic conduction in the cathode.*

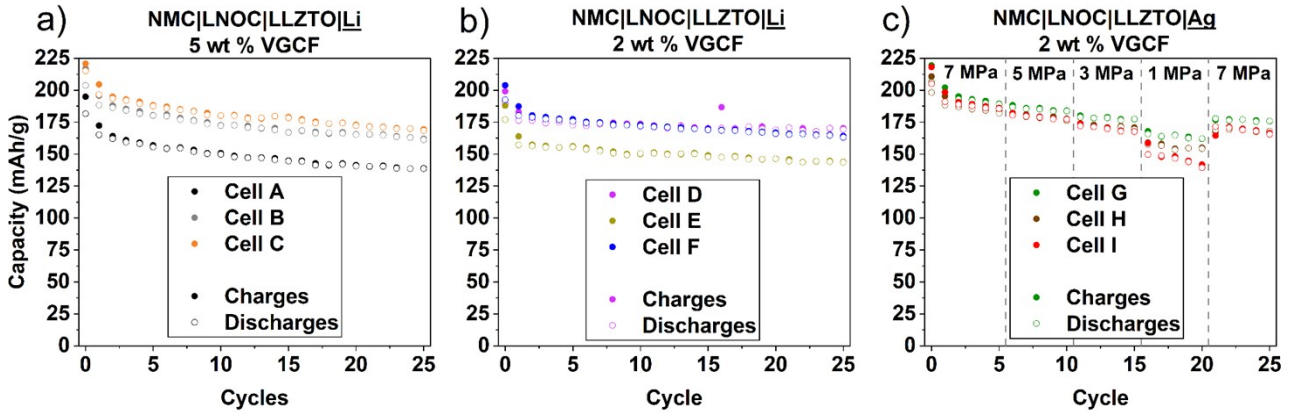

***Figure S18**: Triplicate cycling data of the Li foil full cells with a) 2 wt% VGCF and b) 5 wt% VGCF. c) Triplicate cycling data of the Li reservoir-free cells. Cell G is the cell with the heat treated LLZTO|LNOC interface.*

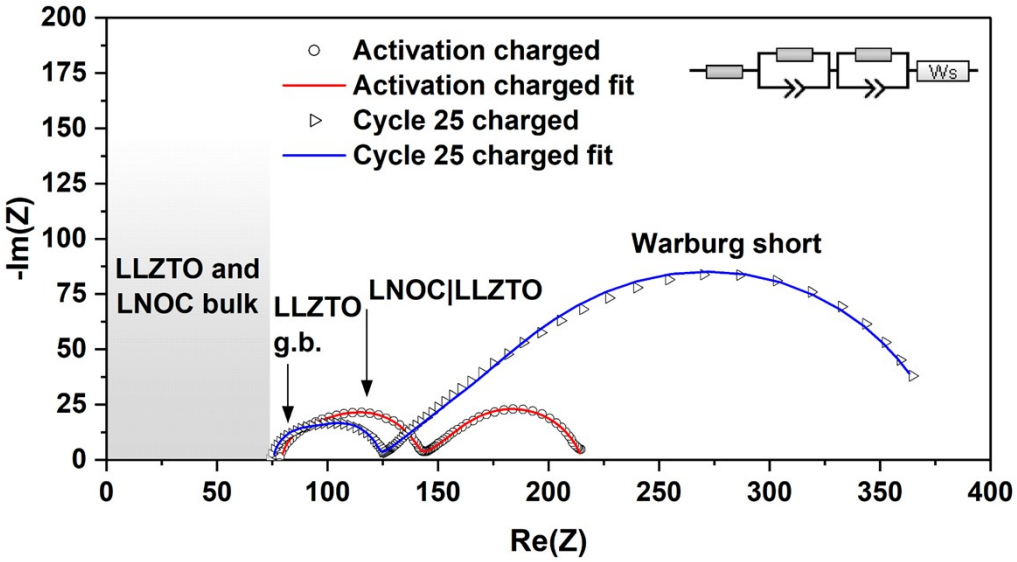

Figure S19: *Nyquist plots and the respective fit of the 5 wt% VGCF full cell in the charged state after the activation cycle and after the 25th cycle. The Nyquist plots were fit with the equivalent circuit R(RQ)(RQ)(Ws).*

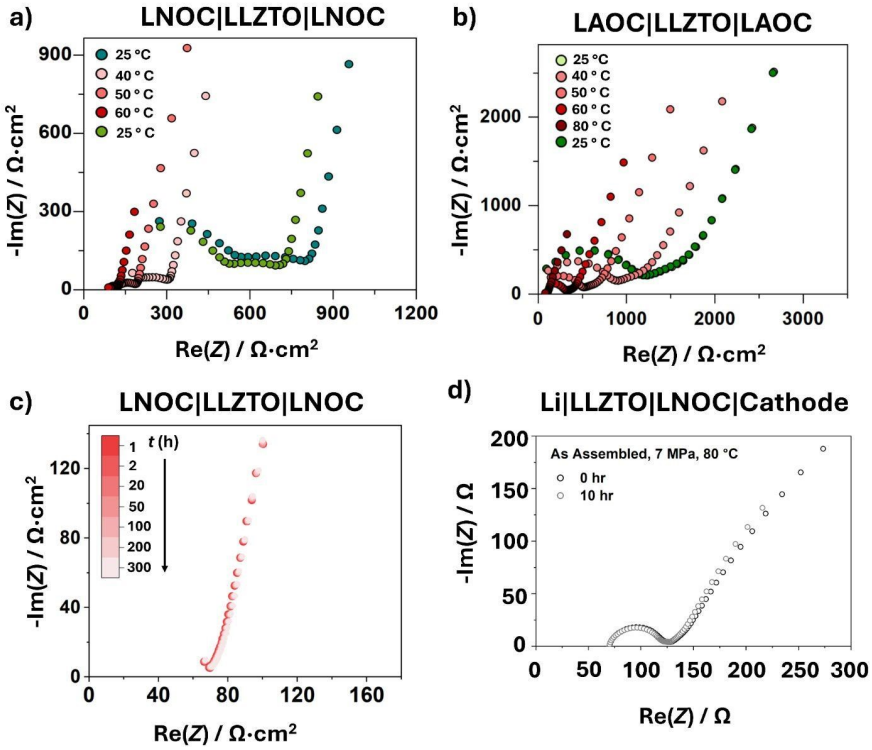

Figure S20: *Nyquist plots corresponding to EIS data collected starting at 25 °C, followed by a hold at 60 °C for 5 hours, and re-equilibration at 25 °C of bilayer symmetric cells, (a) LNOC|LLZTO|LNOC, and (b)LAOC|LLZTO|LAOC; (c) Nyquist plots of a LNOC|LLZTO|LNOC bilayer symmetric cell at 55 MPa and 60 °C held for 300 hours. No change in the Nyquist plots after dwelling at 60 °C indicates stability of the LMOC|LLZTO interface. d) Nyquist plots of an assembled full cell at the start and after 10 hours of the warm press step used to form a better LNOC|LLZTO contact which decreases the cell resistance.*

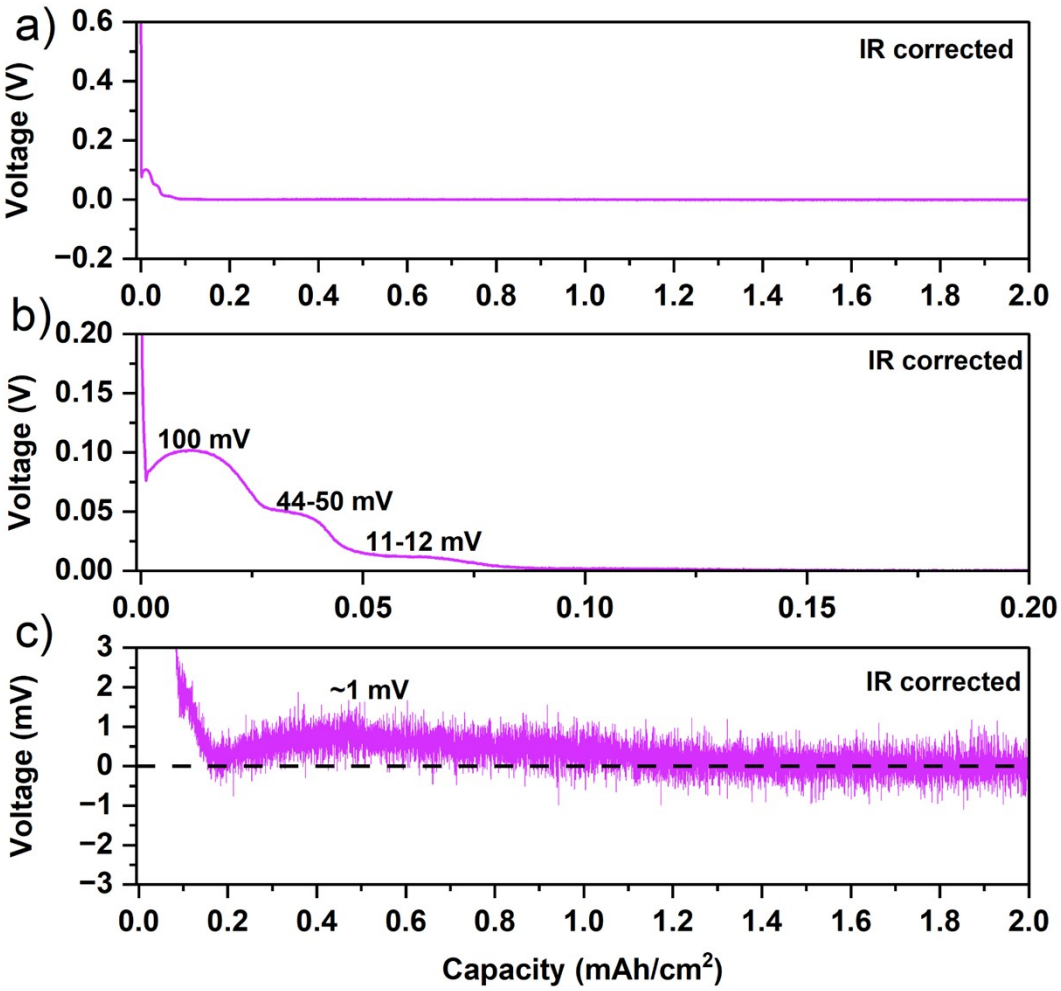

Figure S21: *The first plating of Li during the activation cycle in a Li|LLZTO|Ag half-cell. To identify the plateaus, the plating voltage has been IR corrected to account for the IR drop. Three plateaus at 100 mV, 44-50 mV, and 11-12 mV are noticed within the first 0.1 mAh cm² of plated Li. A fourth plateau is almost unnoticeable at a voltage of ~1 mV. The voltage of the regions between the plateaus agree well with the computational work on the Li-Ag system by Thomas et al.[6] Based on Thomas et al. work, the three initial plateaus with increasing plated Li are attributed to Li_8Ag_3, Li_3Ag, and $Li_{11}Ag_2$. A Li-Ag alloy was identified by Thomas et al. at 2 mV with a body-centered cubic structure although the composition was not determined. This phase is observed but not identified at this time.*

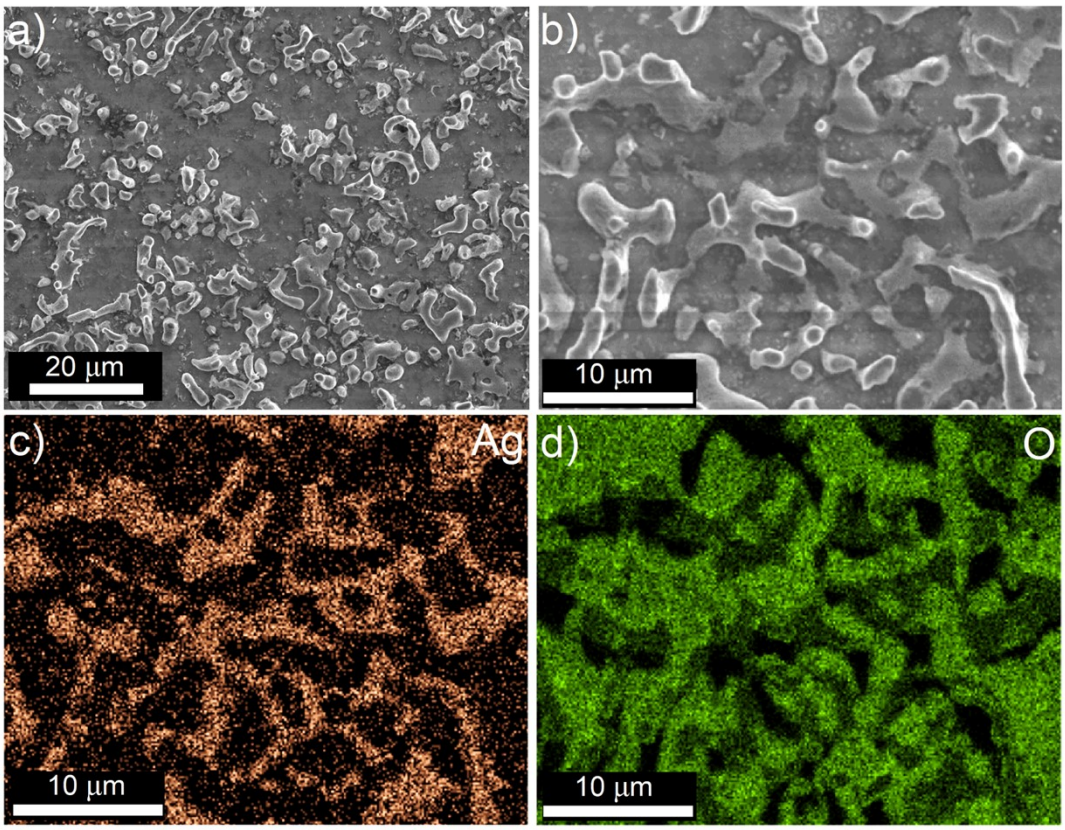

Figure S22: *a,b) SEM images of the Ag on the LLZTO surface cycling in the Li|LLZTO|Ag half-cell. c) Silver (Ag) and d) oxygen (O) elemental mapping from EDX of the region shown in b). The Ag mapping shows the structures on the LLZTO are Ag rich regions.*

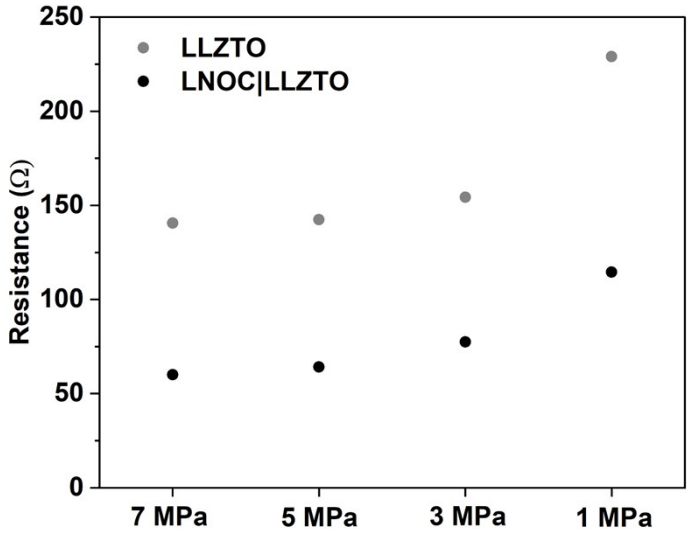

Figure S23: *The LLZTO and LNOC|LLZTO interface resistance in the Li reservoir-free full cell at each pressure.*

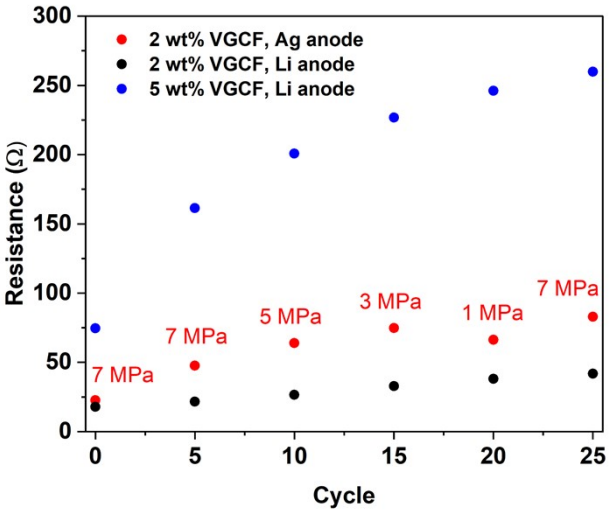

***Figure S24**: A comparison of the low frequency resistance with 2 wt% VGCF in cathode with Ag and Li anode cells and a 5 wt% VGCF in cathode with Li anode cell. The pressure for the Li anode cells was constant at 7 MPa.*

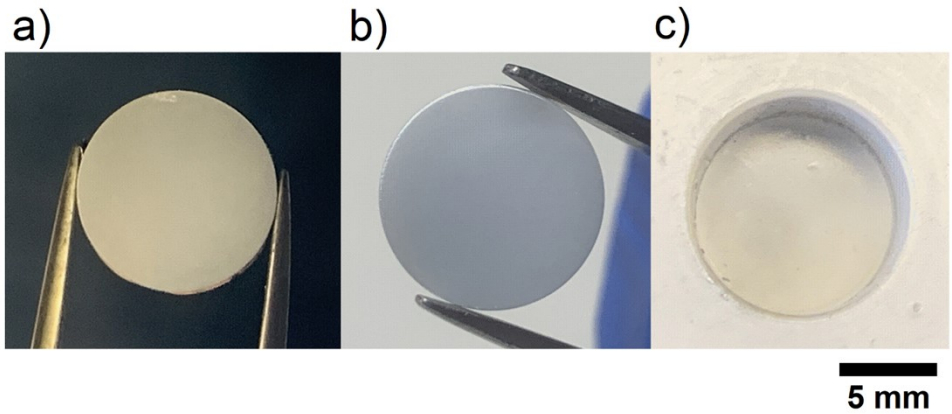

***Figure S25**: Li reservoir-free full cell after cycling. The a) Li side and b) LNOC side. After cycling the LLZTO was removed from the cell. As there was not 100% efficiency during cycling, there was residual Li on the LLZTO. To view the LLZTO surface and confirm there were no dendrites, the Li-Ag on the LLZTO was wiped with ethanol. No dendrites can be observed c) The LNOC interlayer after cycling.*

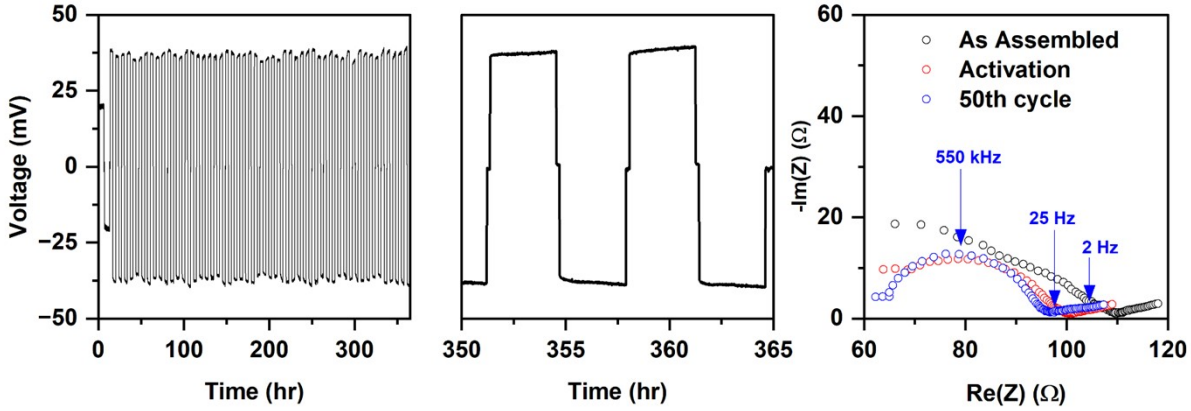

***Figure S26**: A Li|LLZTO|Li symmetric cell cycled at 7 MPa and 60 °C. The cell was cycled at 0.314 mA/cm^2 (corresponding to C/10 for the full cell) for one cycle and then the current was increased to 0.628 mA/cm^2 (corresponding to C/5).*

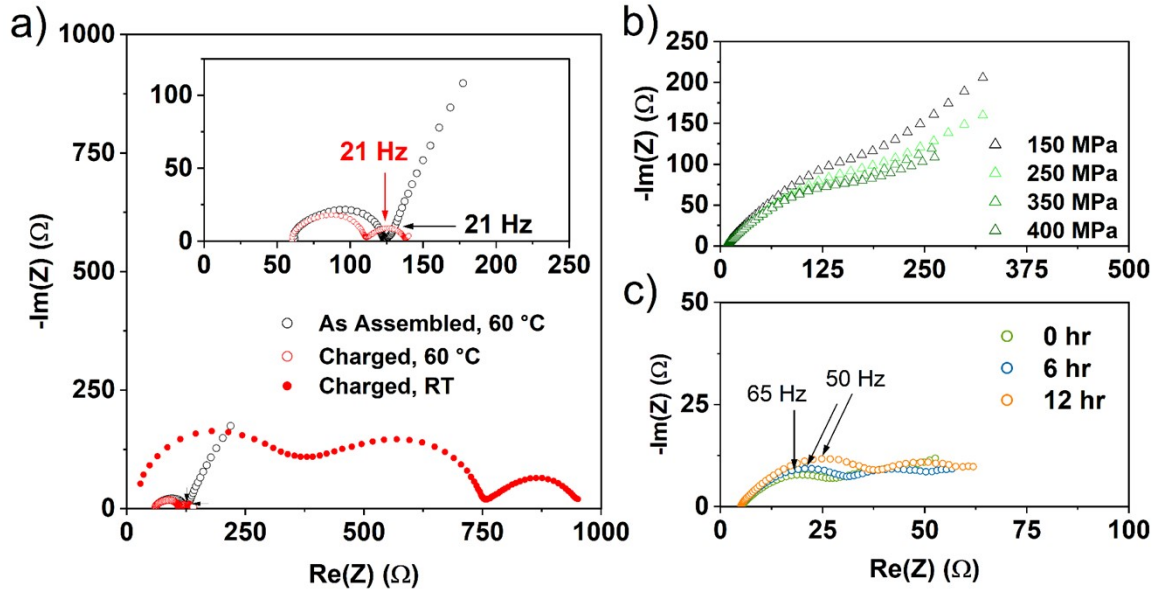

***Figure S27**: A full cell of NMC|LNOC|LLZTO|Li was assembled and charged to 4.3 V. a) The Nyquist plots of the cell as assembled, after charging to 4.3 V, and then cooling to room temperature. Due to the lack of adhesion between the LNOC and LLZTO, the LLZTO|Li was easily removed from the full after cooling, leaving a NMC|LNOC layer with the NMC at 100% SOC. Fresh composite cathode powder was then added to the exposed LNOC side. b) Nyquist plot after adding fresh composite cathode powder and densifying the NMC|LNOC|NMC cell at increasing fabrication pressure. c) Nyquist plot of the symmetric cell over time after heating to 80 °C*

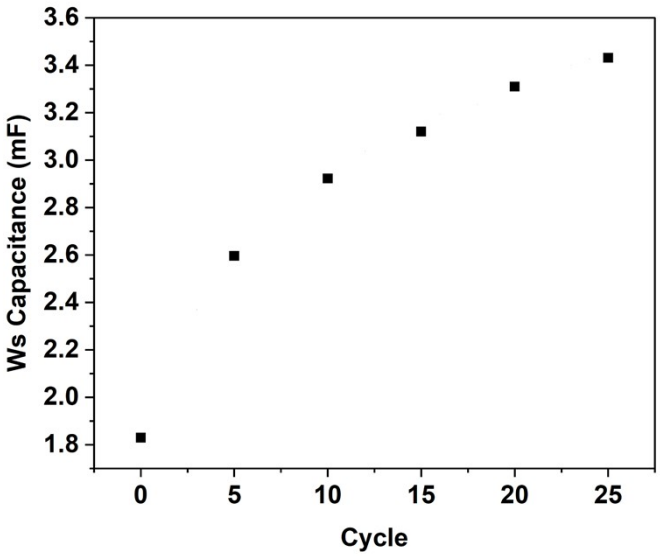

Figure S28: *Capacitance of the Warburg short element from* ***Fig. 5***.

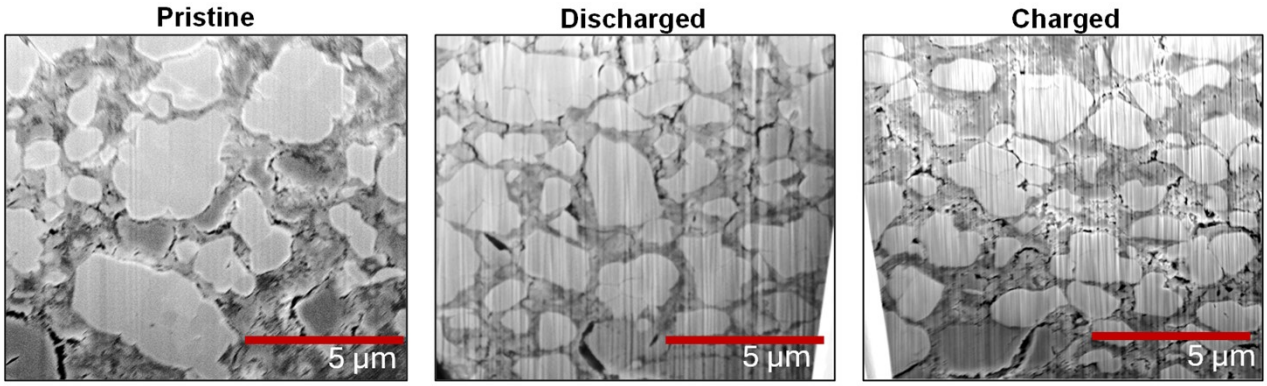

Fig. S29: *a) Pristine composite cathode after densifying at 370 MPa. b) Composite cathode in the discharged state after 25 cycles. c) Composite cathode in the charged state after 25 cycles.*

Table S1: *Ultrasonic measurements for LMOCs. (v = Poisson's ratio; E = elastic modulus; G = shear modulus; K = bulk modulus)*

	v	v (std dv)	E (GPa)	E (std dv)	G (GPa)	G (std dv)	K (GPa)	K (std dv)
LTOC	0.13	0.030	7.1	0.365417	3.1	0.239	3.2	0.117
LNOC	0.19	0.002	8.2	0.645991	3.5	0.272	4.5	0.347
LACO	0.31	0.011	7.6	0.673867	2.9	0.283	6.6	0.194

***Table S2**: Comparison between the transport properties of the processes found in bilayer symmetric cells (LMOCs|LLZTO|LMOCs) at 25 °C and 55 MPa stack pressure with n=3. LLZTO roughness (Sq = 120-150 nm)*

Cell assembly	R_{HE} / Ω cm²	C / μF cm⁻²	τ / μs	$f_{(H\text{-}E)}$ / kHz
LNOC|LLZTO|LNOC	150 ± 24	3.6 ± 0.1	270 ±15	3.7
LTOC|LLZTO|LTOC	155 ± 10	2 ± 0.2	310 ± 10	5.2
LAOC|LLZTO|LAOC	35 ± 5	7 ± 2	245 ± 20	4.1

Σ (Std. dev.) = $\sqrt{(\Sigma(x - \bar{x})^2 / N)}$

x	Each data value
$\bar{x}$	Mean (average) of data
N	Total number of data points
n	Sample size (n=3)

Brug's equation

$$C = \left[\frac{Q}{R^{1-\alpha}}\right]^{\frac{1}{\alpha}}$$

C	Capacitance
Q and α	Capacity and form factor
R	Resistance
n	Sample size (n=3)

$$\tau = R.C = R.\frac{(Q.R)^{\frac{1}{\alpha}}}{R}$$

τ	Time constant

***Table S3**: Hetero-electrolyte interface resistance, activation energy, and time constant values after the surface treatment of LLZTO discs.*

Cell assembly LNOC|LLZTO|LNOC	$R_{H\text{-}E}$ / Ω cm²	C / μF cm⁻²	$E_{a\,(H\text{-}E)}$ / eV
MP	150 ± 24	3.6 ± 0.1	0.52 ± 0.01
HT	37 ± 25 (outlier = 85)	6.9 ± 3	0.49 ± 0.03
14.6 M H_3PO_4	41 ± 15	2.26 ± 1.2	0.54 ± 0.01
1 M H-Cl	250 ± 50	1.9 ± 0.4	0.56 ± 0.02

References

1. Y. Tanaka, K. Ueno, K. Mizuno, K. Takeuchi, T. Asano and A. Sakai, *Angew Chem Int Ed*, 2023, **62**, e202217581.
2. G. Han, B. Kinzer, R. Garcia-Mendez, H. Choe, J. Wolfenstine and J. Sakamoto, *Journal of the European Ceramic Society*, 2020, **40**, 1999–2006.
3. T. Krauskopf, H. Hartmann, W. G. Zeier and J. Janek, *ACS Appl. Mater. Interfaces*, 2019, **11**, 14463–14477.
4. M. Palmer, L. Qian, V. K. Singh, L. Merola, E. Carlson, C. Haslam, J. Janek, L. F. Nazar and J. Sakamoto, *Solid State Ionics*, 2025, **428**, 116948.
5. A. D. Pelton, *Bulletin of Alloy Phase Diagrams*, 1986, **7**, 223–228.
6. J. Thomas, S. S. Behara and A. Van Der Ven, *Chem. Mater.*, 2024, acs.chemmater.4c01903.
7. L. Merola, V. K. Singh, M. Palmer, J. K. Eckhardt, S. L. Benz, T. Fuchs, L. F. Nazar, J. Sakamoto, F. H. Richter and J. Janek, *ACS Appl. Mater. Interfaces*, 2024, acsami.4c11597.

8. A. Sharafi, H. M. Meyer, J. Nanda, J. Wolfenstine and J. Sakamoto, *Journal of Power Sources*, 2016, **302**, 135–139.
9. M. Papakyriakou, M. Lu, Y. Liu, Z. Liu, H. Chen, M. T. McDowell and S. Xia, *Journal of Power Sources*, 2021, **516**, 230672.
10. S. Wang, E. Barks, P.-T. Lin, X. Xu, C. Melamed, G. McConohy, S. Nemšák and W. C. Chueh, *Chem. Mater.*, 2024, **36**, 6849–6864.
11. H. Huo, Y. Chen, N. Zhao, X. Lin, J. Luo, X. Yang, Y. Liu, X. Guo and X. Sun, *Nano Energy*, 2019, **61**, 119–125.